Sampling, separation, and quantification of *N*-acyl homoserine lactones from marine intertidal sediments

Frederike Stock [1a] Emilio Cirri [2,3a] Samarasinghe Gunasekara Liyanage Ishari Nuwanthi,[4]
Willem Stock,[1] Nico Ueberschaar,[5] Sven Mangelinckx,[4] Georg Pohnert [2*b] Wim Vyverman[1b]

[1]Laboratory of Protistology and Aquatic Ecology, Department of Biology, Ghent University, Ghent, Belgium
[2]Institute for Inorganic and Analytical Chemistry, Friedrich Schiller University Jena, Jena, Germany
[3]Leibniz Institute on Aging Fritz-Lipmann Institute Jena, Beutenbergstrasse 11, Jena, Germany
[4]SynBioC, Department of Green Chemistry and Technology, Faculty of Bioscience Engineering, Ghent University, Ghent,
Belgium
[5]Mass Spectrometry Platform, Friedrich Schiller University Jena, Jena, Germany

Abstract

N-acyl homoserine lactones (AHLs) are molecules produced by many Gram-negative bacteria as mediators of cell-cell signaling in a mechanism known as quorum sensing (QS). QS is widespread in marine bacteria regulating diverse processes, such as virulence or excretion of polymers that mediate biofilm formation. Associated eukaryotes, such as microalgae, respond to these cues as well, leading to an intricate signaling network. To date, only very few studies attempted to measure AHL concentrations in phototrophic microbial communities, which are hot spots for bacteria-bacteria as well as microalgae-bacteria interactions. AHL quantification in environmental samples is challenging and requires a robust and reproducible sampling strategy. However, knowing about AHL concentrations opens up multiple perspectives from answering fundamental ecological questions to deriving guidelines for manipulation and control of biofilms. Here, we present a method for sampling and AHL identification and quantification from marine intertidal sediments. The use of contact cores for sediment sampling ensures reproducible sample surface area and volume at each location. Flash-freezing of the samples with liquid nitrogen prevents enzymatic AHL degradation between sampling and extraction. After solvent extraction, samples were analyzed with an ultra-high performance liquid chromatography-high resolution mass spectrometry (UHPLC-HRMS) method that allows to baseline-separate 16 different AHLs in less than 10 min. The sensitivity of the method is sufficient for detection and quantification of AHLs in environmental samples of less than 16 cm^3.

N-acyl homoserine lactones (AHLs) are a class of molecules which are produced by many Gram-negative bacteria during a signaling process called quorum sensing (QS) (Waters and Bassler 2005). Structurally, the lactone of the amino acid homoserine is functionalized via an amide bond with acyl chains that differ in their degree of saturation, length, and chemical functionalization, such as hydroxyl- and carbonyl-groups (Waters and Bassler 2005). AHLs can be synthesized by

three different protein families, the best studied group being LuxI-type synthases (utilized by Alpha-, Beta-, and Gammaproteobacteria) which use *S*-adenosyl-L-methionine and an acyl-acyl carrier protein as substrate (Parsek et al. 1999; Frederix et al. 2011). Much less is known about the enzymatic synthesis of AHLs by LuxM- and HdtS-type synthases which have only been identified in very few bacterial species (Li and Nair 2012). LuxM-type synthases are found in *Vibrio* and related species, for example, LuxM (*Vibrio harveyi*), AinS (*V. fischeri*), and VanM (*V. anguillarum*) (Frederix et al. 2011). HdtS-type synthases were first discovered in *Pseudomonas fluorescens* and their mechanisms of AHL synthesis remain uncharacterized (Churchill and Chen 2011). After synthesis and release, AHLs re-enter bacterial cells and bind to LuxR type receptors which control expression of QS regulated genes (Waters and Bassler 2005). This mechanism allows bacteria to coordinate gene expression, which eventually leads to a behavioral change in the population (Waters and Bassler 2005).

QS has been predominantly investigated in pathogens such as *Pseudomonas aeruginosa*, but AHL-based QS also occurs in marine environments (Wagner-Döbler et al. 2005; Doberva et al. 2015; Hmelo 2017). For instance, AHL production was confirmed in 39 out of 67 marine Alphaproteobacteria using a screening with bacterial reporter strains followed by gas chromatography-mass spectrometry (GC-MS) analysis (Wagner-Döbler et al. 2005). This finding was in line with an in silico analysis of the Global Ocean Sampling metagenome database where several *luxI* homologues were identified in microplankton samples suggesting that QS signaling is widespread in marine bacteria (Doberva et al. 2015). AHL signaling also plays an important role in shaping algae-bacteria interactions (Joint et al. 2007; Yang et al. 2016; Zhou et al. 2016; Stock et al. 2019). For example, AHLs can influence diatom/bacteria-biofilm formation (Yang et al. 2016), control zoospore settlement of the green seaweed *Ulva* (Joint et al. 2007), and inhibit diatom growth (Stock et al. 2019). In addition, some microalgae are able to interfere with bacterial QS by mimicking AHLs (Teplitski et al. 2004) or degrading them (Natrah et al. 2011; Syrpas et al. 2014).

Given their ecological role in intra- and interspecies communication, the qualitative and quantitative assessment of AHLs in environmental samples has been a desirable goal for many years. Until recently, the most common tool for AHL identification was screening with bacterial reporter strains that phenotypically respond to exogenous AHLs, for example, by emitting luminescence (Winson et al. 1998). However, only a few reporter strains exist that are able to detect a broad range of AHLs (Zhu et al. 2003), while most reporter strains have a narrow substrate tolerance, which requires utilization of different strains to detect structurally diverse AHLs (Steindler and Venturi 2007; Sun et al. 2018). Although this technique is quite sensitive, it is not suitable for AHL quantification. Given these limitations and technological advances in analytical chemistry, AHL detection by bacterial reporter strains is nowadays often used in combination with, or replaced by, GC-MS and liquid chromatography-mass spectrometry (LC-MS) methods (Huang et al. 2007; Decho et al. 2009; Wang et al. 2017; Sun et al. 2018). Still, the wide range of polarity, the low concentrations in environmental samples and the often complex matrix make a quantitative assessment of AHLs in field samples challenging. These obstacles explain the scarcity of studies that have attempted to quantify AHLs in microbial mats (Decho et al. 2009), sludge from bioreactors (Wang et al. 2017; Sun et al. 2018), subtidal biofilms (Huang et al. 2007), and soils (Sheng et al. 2017).

In the present study, we aimed to quantify AHLs in marine intertidal sediments that form hotspots for diatom-bacteria interactions. Although previous studies have described the extraction and quantification of AHLs from biofilms, sampling and AHL quantification strategies were not suitable for intertidal sediments. For instance, a previous study measured AHL concentrations in subtidal biofilms and used petri dishes for sampling that are administered into the environment and collected after biofilm formation, thereby selecting for settlers on the artificially introduced surface (Huang et al. 2007). We aimed to sample intertidal sediments without introducing such bias; however, a sampling approach with controlled sampling surface and depth was needed because the thin euphotic zone of the sediment typically extends approximately 2 mm below the sediment surface (Underwood and Kromkamp 1999). The biomass dynamics in this upper compartment of the sediment are independent of those of the deeper sediment which makes this fraction particularly interesting for ecological studies (Herlory et al. 2004).

Regarding methods for the chromatographic separation of AHLs, ultra-high performance liquid chromatography-tandem mass spectrometry (UHPLC-MS/MS) is suitable to separate and quantify several AHLs in a short time (up to 19 AHLs in 9 min in Ortori et al. 2011, 13 AHLs in 6 min in Wang et al. 2017), but these protocols failed to achieve a baseline separation for most compounds. Moreover, to date no study has exploited the advantage of high-resolution mass spectrometry (HRMS) and the high sensitivity of the Orbitrap analyzer to identify and quantify AHLs in environmental samples.

For AHL quantification, AHL concentration was mostly normalized to biofilm or sediment weight after air-drying (Sheng et al. 2017) or freeze-drying (Decho et al. 2009; Wang et al. 2017). However, previous studies predominantly sampled biofilm from hard substrates resulting in biofilm samples which consisted almost entirely of organic matter (Huang et al. 2007; Wang et al. 2017). In contrast, samples collected in the present study contained a lot of sediment; hence, weight of dried samples was determined by sediment weight rather than biomass.

In the present study, we report a reproducible sampling strategy for marine intertidal surface sediments by using contact cores. This method has already been used to sample microphytobenthic biomass for DNA and pigment extraction and was successfully adapted for AHL quantification. A fast AHL extraction method using dichloromethane was modified from Decho et al. (2009). We also established a UHPLC-MS protocol that allowed separation of 19 AHL standards (16 of which were baseline separated) using UHPLC-HRMS/MS (partially adapted from Sun et al. 2018) covering a wide range of polarities within less than 10 min.

Materials and procedures

Reagents

AHL standards used for UHPLC-HRMS/MS method development and internal standards were synthesized in-house. Briefly, even numbered *N*-hexanoyl-homoserine lactone (C6) to *N*-tetradecanoyl-homoserine lactone (C14) and *N*-3-oxohexanoyl-homoserine lactone (OXO6) to *N*-3-oxotetradecanoyl-homoserine lactone (OXO14) were synthesized according to Hodgkinson et al. (2011) and synthesis

of *N*-3-hydroxyhexanoyl-homoserine lactone (OH6) to *N*-3-hydroxytetradecanoyl-homoserine lactone (OH14), including *N*-3-hydroxytridecanoyl-homoserine lactone (OH13), was performed as described in Cao et al. (1995). *N*-3-oxononanoyl-homoserine lactone (OXO9) was synthesized as described in Syrpas et al. (2014) and deuterated standards *N*-[3-^{2}H$_2$]-octanoyl-homoserine lactone (C8D) and *N*-[3-^{2}H$_2$]-dodecanoyl homoserine lactone (C12D) were prepared according to Ruysbergh et al. (2016). As internal standards (ISTDs) C8D, C12D as well as OXO9 and OH13 were selected to cover all possible polarities. An overview of all AHL standards can be found in Table 1 and Fig. 1.

Acetone (Chem-Lab, Belgium), dichloromethane (DCM) (Merck, Belgium), and methanol (Chem-Lab, Belgium) used in this study were high-performance liquid chromatography (HPLC) grade. Acetonitrile (ACN) (HiPerSolv Chromanorm, VWR, Germany) was UHPLC grade. Acetic acid (99.8%) was purchased from Merck (Belgium) and formic acid for LC-MS (LiChropur®) from Merck (Germany).

Sampling of intertidal sediments

Intertidal sediments were sampled in February and April 2018 during low tide on the mudflats of Paulinapolder close to Terneuzen, Netherlands (51°20′N, 003°43′E, Supporting Information Fig. S1). All samples were taken in the morning and early afternoon. During both campaigns, six randomly chosen locations (plots) with visibly different sediment composition were sampled. For collection, an in-house manufactured sampling frame was used to ensure that replicates for one plot were taken within a defined surface area of 2500 cm^2 (Fig. 2a). The metal frame (50 cm × 50 cm) was placed directly on the sediment, and a removable wooden grid was positioned on top of the metal frame with threads dividing the area in 5 × 5 squares of 10 cm × 10 cm.

To collect the surface sediment layers corresponding to the photic zone within the sediment, we used contact cores made out of aluminum to ensure that the depth and surface area were the same in each replicate. Sampling with contact cores is already used for the collection of microphytobenthos for pigment and DNA extractions (Maris and Meire 2017). It proved to be robust, easy to execute in the field and it was reproducible over the two sampling campaigns. For AHL quantification, sediments were collected using large contact cores (manufactured in house) with a diameter of 5 cm (bottom depth 2 mm) (for more details, see Fig. 2b,c). These same samples were used for total organic matter (TOM) content and grain size analysis. Smaller contact cores (manufactured in house) with a diameter of 2.5 cm (bottom depth 2 mm) were used to collect samples for pigment extraction (Fig. 2a).

For sample collection, contact cores were pressed onto the sediment with the bottom site (2 mm of inner edge) facing downward while liquid nitrogen was poured into the upper part of the core. After liquid nitrogen had evaporated, frozen sediment remained attached to the bottom site of the contact

Table 1. Full names and abbreviations of all AHL standards and internal standards (ISTDs, marked with ∗) used in this study. The right column indicates which ISTD was used for quantification of each target AHL. ISTDs were assigned based on retention time; OXO9 and OH13 were not used for quantification.

Name	Abbreviation	Internal standard
N-3-oxohexanoyl homoserine lactone	OXO6	C8D
N-3-hydroxyhexanoyl homoserine lactone	OH6	C8D
N-hexanoyl homoserine lactone	C6	C8D
N-3-oxooctanoyl homoserine lactone	OXO8	C8D
N-3-hydroxyoctanoyl homoserine lactone	OH8	C8D
N-octanoyl homoserine lactone	C8	C8D
N-[3-^{2}H$_2$]-octanoyl homoserine lactone∗	C8D	—
N-3-oxononanoyl homoserine lactone∗	OXO9	—
N-3-oxodecanoyl homoserine lactone	OXO10	C8D
N-3-hydroxydecanoyl homoserine lactone	OH10	C8D
N-decanoyl homoserine lactone	C10	C12D
N-3-oxododecanoyl homoserine lactone	OXO12	C12D
N-3-hydroxydodecanoyl homoserine lactone	OH12	C8D
N-dodecanoyl homoserine lactone	C12	C12D
N-[3-^{2}H$_2$]-dodecanoyl homoserine lactone∗	C12D	—
N-3-hydroxytridecanoyl homoserine lactone∗	OH13	—
N-3-oxotetradecanoyl homoserine lactone	OXO14	C12D
N-3-hydroxytetradecanoyl homoserine lactone	OH14	C12D
N-tetradecanoyl homoserine lactone	C14	C12D

core and could be taken out of the ground. Subsequently, residual sediment stuck to the bottom of the core was leveled with a knife until the metal edge became visible. This way a frozen sediment disk with a uniform thickness of 2 mm was obtained. Sediment disks were taken randomly within the sampling plot and large sediment disks (ø 5 cm) were collected in plastic bags while small sediment disks (ø 2.5 cm) were collected in aluminum cans (Rotilabo, ø 3 cm). For TOM content, grain size analysis, and AHL quantification, four large sediment disks were pooled per replicate. For pigment analysis,
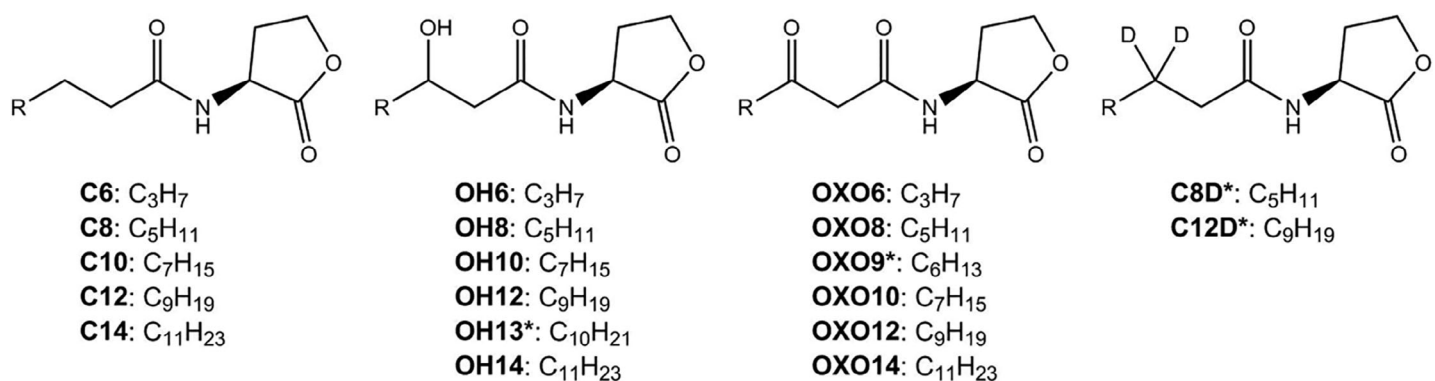
Fig 1. AHL standards used in this study. Internal standards are marked with "*."

C6: C_3H_7
C8: C_5H_{11}
C10: C_7H_{15}
C12: C_9H_{19}
C14: $C_{11}H_{23}$

OH6: C_3H_7
OH8: C_5H_{11}
OH10: C_7H_{15}
OH12: C_9H_{19}
OH13*: $C_{10}H_{21}$
OH14: $C_{11}H_{23}$

OXO6: C_3H_7
OXO8: C_5H_{11}
OXO9*: C_6H_{13}
OXO10: C_7H_{15}
OXO12: C_9H_{19}
OXO14: $C_{11}H_{23}$

C8D*: C_5H_{11}
C12D*: C_9H_{19}

Contact core with 5 cm diameter
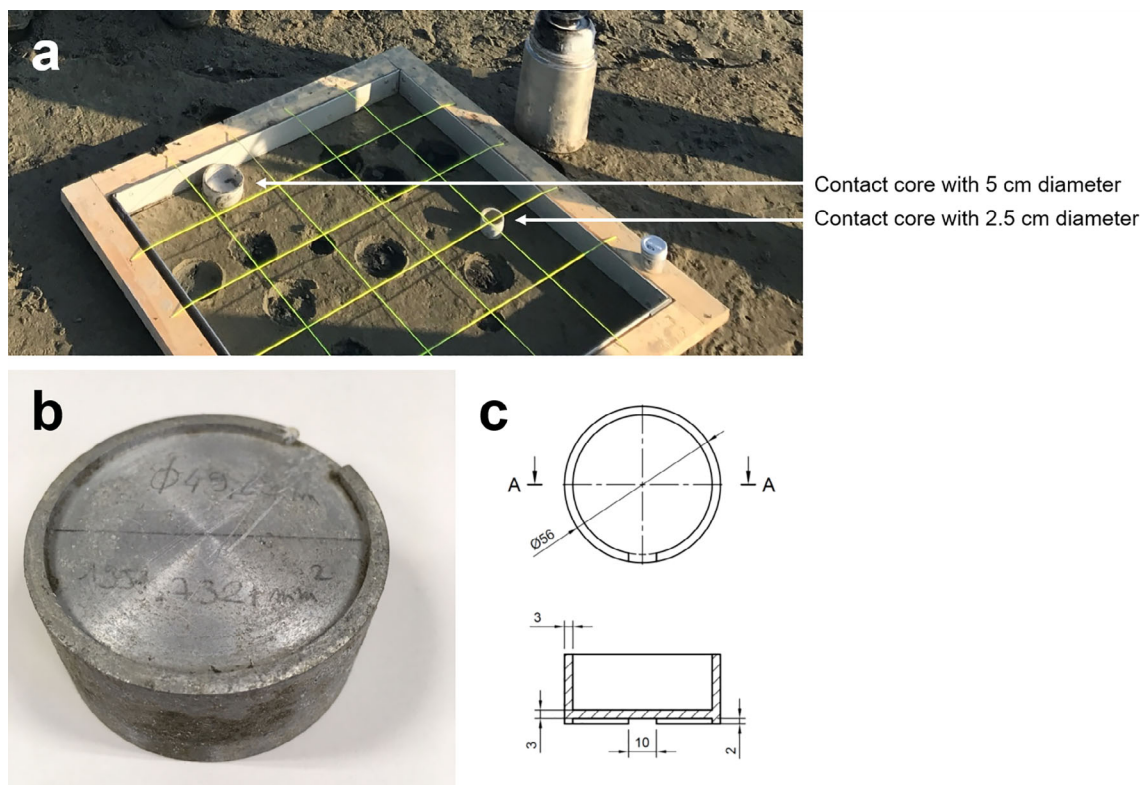Contact core with 2.5 cm diameter

Fig 2. Sampling devices used in this study. (**a**) Sampling grid consisting of a metal frame (0.5 × 0.5 m) on which a wooden frame is placed with threads dividing the area in squares of 10 × 10 cm. Contact cores for sediment sampling are indicated with white arrows. (**b**) Photograph of a contact core (ø 5 cm) with the bottom site facing upward. (**c**) Technical drawing of a contact core (ø 5 cm) with top and side view as it was used for AHL extraction, organic matter, and grain size analyses. "A" indicates the section for the side view below, dimensions are provided in millimeter. The 10 mm gap in the side view indicates the site where the knife can be inserted to remove the frozen sediment from the core. It should be noted that smaller contact cores (ø 2.5 cm) were used for pigment extraction.

three small disks were combined into one replicate. In total, three replicates were collected with large and small contact cores in each plot (Fig. 3). Plastic bags and aluminum cans containing the sediment samples were immediately placed on dry ice and maintained frozen for the whole transportation back to the laboratory before they were stored at −80°C to prevent AHL degradation.

Sample preparation

Prior to freeze-drying, all large sediment disks (ø 5 cm) from each replicate were transferred into petri dishes and covered with aluminum foil to avoid spilling of samples. Small sediment disks (ø 2.5 cm) for pigment extraction were freeze-dried in their respective aluminum cans. All samples were freeze-dried (Lyotrap, LTE Scientific, Great Britain, UK) for 24–48 h
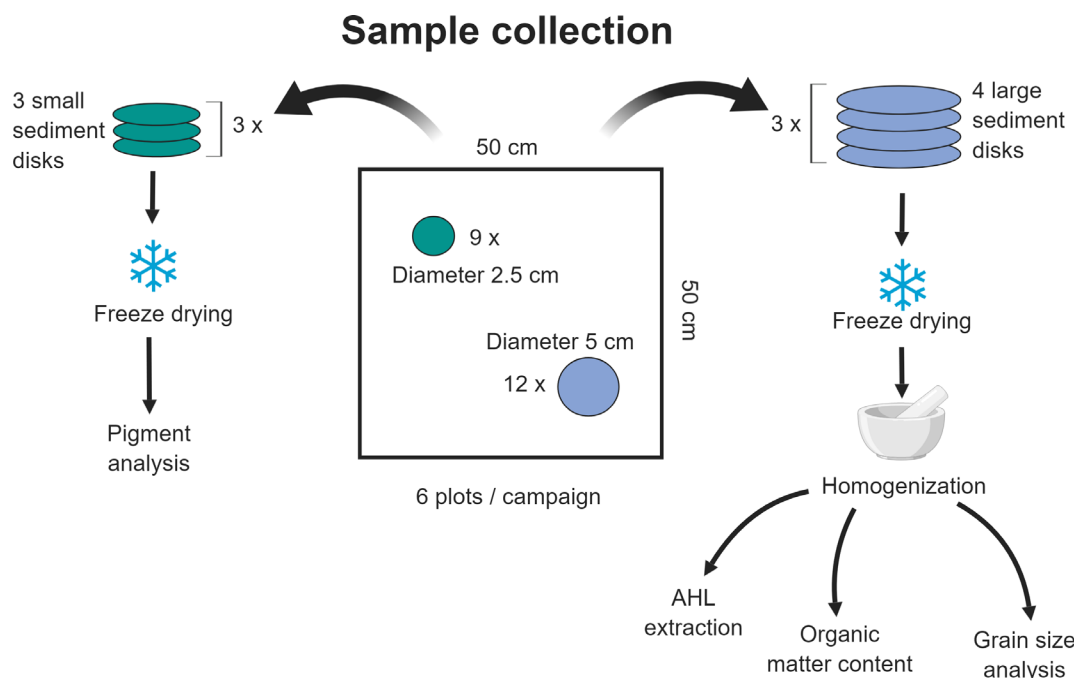
Sample collection

Fig 3. Schematic overview of sample collection and processing. Biofilm samples were collected within a plot of 50 cm × 50 cm with large contact cores (ø 5 cm, blue) and small contact cores (ø 2.5 cm, green). One sample for pigment extraction consisted of three small sediment disks, while one sample for AHL extraction, organic matter content, and grain size analysis consisted of four large sediment disks. In total, three samples were taken with large and small contact cores in each plot. Six plots were sampled per sampling campaign.

in the dark. Afterward, large sediment disks were gently homogenized with a pestle and aliquoted for AHL extraction (10 g), TOM analysis (10 g), and grain size measurements (rest).

Pigment extraction, separation, and quantification

Pigment extraction was conducted under red light to prevent light-induced degradation. First, 10 mL of acetone : water (9 : 1 v:v) was added to each sediment sample in its respective sampling container. Subsequently, samples were sonicated using a point sonicator (Sonics Vibra-Cell™) for 30 s at 40 Hz and then allowed to settle for 2 h in the dark. Before HPLC analysis, samples were filtered with Acrodisc® syringe filters (wwPTFE membrane, 13 mm, pore size 0.2 μm, Pall laboratory—VWR). Pigments were separated on an Agilent 1260 Infinity II system equipped with a diode array detector (1260 Infinity II Diode Array Detector WR, G7115A) using the method described in Van Heukelem and Thomas (2001). Peak detection and integration was done using the software Agilent OpenLab CDS (version C.01.08) and Agilent ChemStation (version A10.02). All chlorophylls and carotenoids were identified based on retention time and their absorbance at 450 nm and/or 665 nm. Pigment quantification was executed with one-point calibration using pigment standards (DHI Denmark). To calculate pigment concentration, a response factor (Rf) was determined by dividing the concentration of the pigment standard ($Conc_{STD}$) by its peak area (AA_{STD}):

$$Rf = \frac{Conc_{STD}}{AA_{STD}}$$

The pigment concentration of the target pigment ($Conc_P$, in mg m^{-2}) in the respective sample was then calculated with:

$$Conc_P = \frac{Rf \times AA_{sample} \times V}{A_c}$$

where AA_{sample} = peak area of the pigment in sample; V = volume of sample used for extraction (0.01 L), and A_c = surface area of three contact cores that made up one sample in m^2 ($3 \times \pi \times 0.0125^2$).

TOM content and grain size analysis of sediments

To determine the TOM content of the freeze-dried sediment, 10 g from each homogenized sediment sample was transferred into ceramic incinerating dishes (model 79MF-7a, Haldenwanger) and weighed on a microbalance (type AX205, Mettler Toledo). Samples were then placed in a furnace (Thermolyne™ furnace type 30400) to incinerate all organic matter at 550°C for 4 h and weighed again. The difference in weight before and after incineration of the organic matter was calculated and expressed as mg g^{-1} (TOM : dry weight).

For grain size analysis, freeze-dried samples were first sieved to remove particles larger than 2 mm before they were analyzed on a Mastersizer 2000 (Malvern®). For sediment

characterization, the median particle diameter was used according to Blott and Pye (2012).

AHL extraction of sediments

Freeze-dried sediment samples were extracted using DCM. The method was based on Decho et al. (2009) with some modifications. Briefly, 30 mL of DCM was added to 10 g of sediment sample. Subsequently, 80 μL of internal standard mixture (C8D, C12D, OH13, and OXO9 dissolved in ACN) was added (final concentration of each ISTD 10 μmol L^{-1}) and samples were mixed on a shaker (100–150 rpm, GFL reciprocating shaker 3006) for 30 min before they were filtered through a GF/F filter (glass microfiber filters, pore size 7 μm, diameter 47 mm, Whatman®) to remove sand and core particles. DCM was evaporated under vacuum (RapidVap, Labconco) and dried samples were taken up in 3×1 mL of ACN. Samples were transferred into 5 mL HPLC glass vials and ACN was evaporated under nitrogen flow at room temperature. Finally, samples were taken up in 50 μL 100% ACN, transferred to 200 μL inserts placed in 1.5 mL glass vials, and stored at -80 °C until measurement.

UHPLC-HRMS/MS Orbitrap measurements

For method development, individual AHL standard stock solutions were prepared in acetonitrile and combined into one standard mixture to a final concentration of 25 μmol L^{-1} for each compound. A separate stock only containing the internal standards C8D, OXO9, OH13, and C12D was prepared in ACN with a final concentration of 6.25 μmol L^{-1} for each ISTD.

The analytical method was partially adapted from Sun et al. (2018). We used the same elution solvents, but in our study a column with a slightly smaller particle size and linear solvent gradient was used, with shorter equilibration times and a higher, adaptive flow rate.

UHPLC-HRMS was carried out using an UltiMate HPG-3400 RS binary pump (Thermo Fisher Scientific, Bremen, Germany) and a WPS-3000 autosampler which was set to 4°C and equipped with a 25 μL injection syringe and a 100 μL sample loop. The injection volume was set to 1 μL for standard measurements and 10 μL for sediment samples. The chromatography column Accucore® C18 column (2.1 $\times$ 100 mm, 2.6 μm particle size, Thermo Scientific, Dreieich, Germany) was kept at 25°C within the column compartment TCC-3200. This column has a smaller particle size compared to the one used by Sun et al. (2018) and allowed a better interaction and separation of the molecules. The elution was carried out using a linear solvent gradient (Table 2), with a shorter equilibration time and a smoother slope compared to the method of Sun et al. (2018). Eluent A was water with 2% acetonitrile and 0.1% formic acid (v : v) (addition of ACN decreases the surface tension of water, therefore increasing sensitivity). Eluent B was ACN with 0.1% formic acid (v : v). The use of these two eluents as binary mobile phase allows us to have a broad

Table 2. Gradient for UHPLC-HRMS measurements. Solvent A was water with 2% of acetonitrile and 0.1% of formic acid, solvent B was acetonitrile with 0.1% of formic acid.

Time (min)	Flow (mL min^{-1})	Solvent B (%)
0.0	0.400	0
0.2	0.400	0
9.7	0.675	100
10.7	0.675	100
11.7	0.400	0

polarity range over the gradient time, suitable to clearly separate both known and potentially unknown AHLs. ACN was chosen due to its high dipole moment and strong elution strength, which slightly reduces retention time for our analytes without compromising peak shape and chromatographic separation of AHLs. The flow, instead of being fixed as in Sun et al. (2018), was adapted throughout the run, from 0.400 mL up to 0.625 mL. This allowed to keep the peak width of late eluting compounds narrow and therefore achieve a better separation.

The UHPLC was coupled to a Thermo Scientific™ Q Exactive plus™ hybrid quadrupole-Orbitrap mass spectrometer equipped with a heated electrospray ionization source. Ionization was performed with a spray voltage of 3 kV and a capillary temperature of 360°C. The sheath gas flow rate was kept at 60 arbitrary units (au); the auxiliary gas rate at 20 au and the sweep gas rate at 5 au. Nitrogen was used as desolvation gas.

For monitoring of AHLs, a full scan measurement in positive mode was used with the following parameters: scanned mass range 50–750 *m/z*, resolution 280,000 (full width at half maximum [FWHM] at *m/z* 200), automatic gain control (AGC) target 3×10^6, and maximum injection time (IT) of 200 ms.

Tandem mass spectrometry (MS^2) experiments were recorded with the following parameters: resolution 35,000 FWHM (*m/z* 200, AGC target 3×10^6, maximum IT of 200 ms, and an isolation window of 0.4 *m/z*). The normalized collision energy (Supporting Information Table S1) was optimized for each AHL by direct infusion of a standard mixture and scanning for the best collision energy to obtain the highest intensity of the characteristic fragment at 102.0549 *m/z* (lactone ring fragment).

Calibration, linearity, stability, and recoveries

From AHL stock solutions, two independent calibration curves were generated for the most abundant AHLs found in sediment samples (C8, C10, and C12). All calibration samples were prepared freshly and independently for an all-in-one calibration. Five calibration solutions contained C8, C10, and C12 in the range from 5×10^{-7} to 1×10^{-5} mol L^{-1} in ACN with C8D and C12D as internal standard (2 μL of a

100 μmol L^{-1} solution in ACN). Additional five calibration solutions contained C10 in the range from 1×10^{-9} to 1×10^{-7} mol L^{-1} in ACN with C12D as internal standard (2 μL of a 10 μmol L^{-1} solution in ACN). All calibration solutions were analyzed by UHPLC-HRMS in five technical replicates. The injection volume was set to 10 μL. The average peak ratio was calculated by dividing the peak area of the analyte by the peak area of the ISTD (C8/C8D, C12/C12D, C10/C12D) and was plotted against the nominal concentration of each analyte for the working range of 1×10^{-9} to 1×10^{-5} mol L^{-1}. Normal distribution, the absence of outliers, and homoscedasticity were verified for the whole concentration range of each calibration curve. A Mandel test was applied to test the linear model against the quadratic model.

Stability of the sample was determined by comparing the AHL content in freshly extracted samples and samples stored at $-20°$C for 6 months. To measure recovery rates, a sample was spiked with the ISTDs and concentrations before and after DCM extraction were compared.

AHL quantification

All UHPLC-HRMS data were acquired and processed with the software Xcalibur™ (version 3.0.63, Thermo Fisher Scientific). Peak areas were first analyzed with the embedded Quan Browser software and each peak was manually checked after integration. Areas of both, the [M + H]$^+$ and the [M + Na]$^+$ peak, were summed for integration. For AHL quantification in the sediment samples, one ISTD (C8D or C12D) was assigned to each target AHL based on retention time (Table 1). However, the degree of deuteration in the pure ISTDs C8D and C12D was not 100% and measurements showed that C8D and C12D contained approximately 1% non-deuterated C8 and C12. Thus, the areas of C8 and C12 identified in the sediment samples were corrected by subtracting 1% of the added standard that falsely contributed to these two analytes.

Relative concentrations of AHL (Conc$_t$ in μmol L^{-1}) were calculated as follows:

$$\text{Conc}_t = \left(\frac{\text{AA}_t}{\text{AA}_{\text{ISTD}}} \times \text{Conc}_{\text{ISTD}} \right)$$

with AA$_t$ = peak area of the target AHL in the sediment sample; AA$_{\text{ISTD}}$ = peak area of corresponding internal standard in the sediment sample, and Conc$_{\text{ISTD}}$ = final concentration of the internal standard in the sediment sample (10 μmol L^{-1}).

Additionally, the AHL content of each sample was normalized to its organic matter content. The amount of a respective AHL was expressed in pmol AHL g^{-1} TOM by following the calculation:

$$M_t = \left(\frac{\text{Conc}_t}{\text{Conc}_{\text{ISTD}}} \times B \times V_s \right) / \text{TOM}$$

with M_t = pmol AHL g^{-1} TOM; B = moles of ISTD injected (10 pmol); V_s = final sample volume (50 μL), and TOM = total organic matter in 10 g of dried sample (in g).

Assessment

Characterization of intertidal sediment

The Paulinapolder site is a highly studied area for intertidal mudflat community dynamics (Brouwer et al. 2015; Decleyre et al. 2015; Bouma et al. 2016). A previous study assessed bacterial diversity of microphytobenthic biofilms in Paulinapolder and demonstrated that the most abundant bacterial phyla were Proteobacteria followed by Bacteroidetes and Cyanobacteria (Decleyre et al. 2015). AHLs are utilized by many members of the Proteobacteria for cell-cell communication (Waters and Bassler 2005), which is why Paulinapolder was chosen as a sampling site. Furthermore, a previous study on microbial mats detected diurnal AHL fluctuations with lower AHL concentrations during the day compared to nighttime, which was suggested to be due to an increase in pH caused by higher photosynthetic rates (Decho et al. 2009). This proposed link between AHL concentration and pH in microbial mats highlights that AHL production and persistence is influenced by environmental parameters.

Environmental parameters monitored for our sampling sites were microphytobenthic biomass, TOM content, and grain size of the sediments (Fig. 4). We collected samples in winter and spring to determine seasonal differences in AHL concentrations. On average, chlorophyll *a* (Chl *a*) concentrations, and hence microphytobenthic biomass, were higher in sediment samples collected in April compared to February (Fig. 4 and Supporting Information Fig. S2). Most samples contained between 20 and 50 mg organic matter g^{-1} dry weight and were classified as very coarse silt (31.25–62.5 μm), very fine sand (62.5–125 μm), and fine sand (125–250 μm) based on particle size (Blott and Pye 2012).

UHPLC-HRMS Orbitrap measurements

For detection and quantification of AHLs, we developed a protocol for UHPLC-HRMS by adapting a previous method from Sun et al. (2018). The new method managed to detect 19 different AHLs in less than 10 min and baseline separation was achieved for 16 out of 19 AHLs (as shown by the total ion current [TIC] chromatogram in Fig. 5). In the only case of incomplete separation (OH10 and C8), extracted ion chromatograms (EICs) allowed an unequivocal quantification (detail in Fig. 5). Direct infusion measurements permitted to optimize collision energy for each compound. The resulting high-resolution MS/MS provided a fundamental tool to confirm the identity of each AHL in sediment samples by combining the retention time information with the high-resolution mass spectra of the different side chain fragments from each molecule. Combination of a full scan mode with
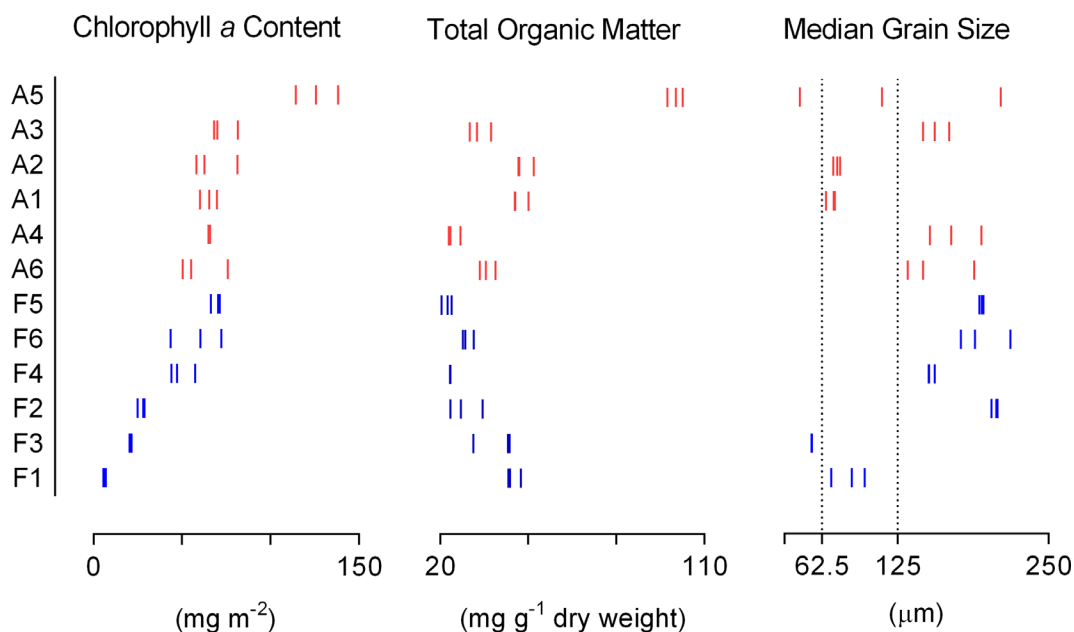
Fig 4. Chlorophyll *a* concentration, TOM content, and median grain size of the sediment samples used in this study. Samples were sorted according to season (blue = February, red = April, numbers indicate the sampled plot) followed by Chl *a* concentration (from high to low). Each bar represents one replicate. Dotted lines represent thresholds for sediment categorization according to Blott and Pye (2012): Very coarse silt (31.25–62.5 μm), very fine sand (62.5–125 μm), and fine sand (125–250 μm).
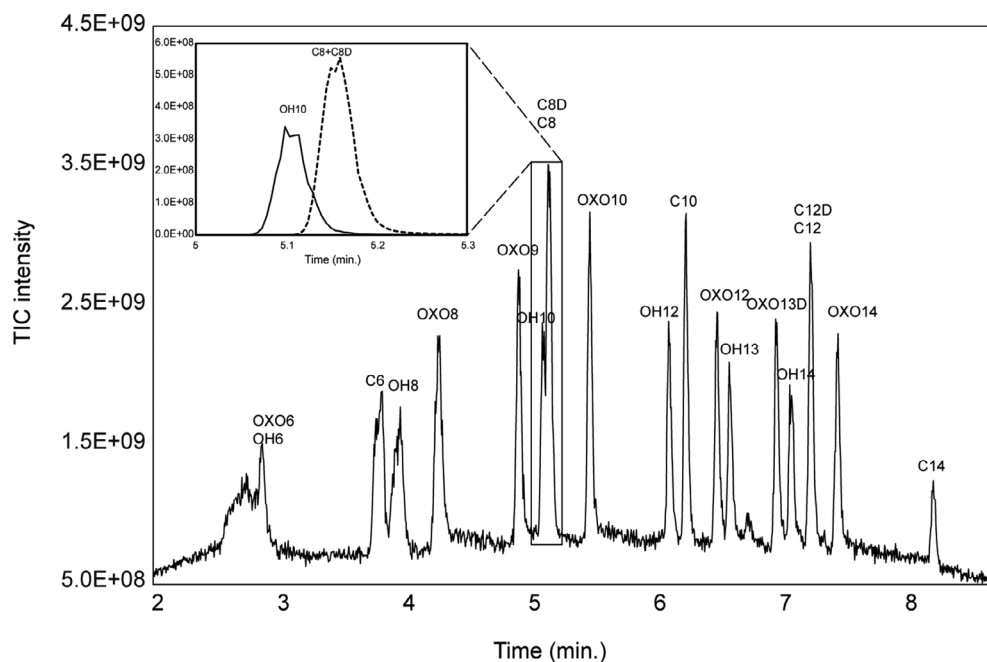

Fig 5. UHPLC-HRMS analysis of AHL standard mixture. The TIC chromatogram shows a baseline separation of 16 out of 19 AHLs. The detail shows the EIC of OH10 and C8. The high resolution allows to identify the two compounds even when baseline separation is not achieved.

an all ion fragmentation (AIF) experiment allows to identify unknown AHLs by searching the accurate mass of the lactone ring fragment (m/z = 102.0549) (Supporting Information Table S1).

Calibration, linearity, stability, and recoveries

All calibration standards passed statistical tests for normal distribution, linearity, and homoscedasticity. As calibration data showed no homoscedasticity over the working range of

5×10^{-7} to 1×10^{-5} mol L^{-1} and in the range of 1×10^{-9} to 1×10^{-7} mol L^{-1} (tested with a one-way ANOVA, $\alpha = 0.05$), a weighted linear regression ($1/y$) was applied for each internal standard (Miller and Miller 2005). No significant differences were determined between the weighted linear and quadratic regressions (Supporting Information Fig. S3). The weighted linear model was thus accepted and used for quantification. Remeasurement of samples which were stored for 6 months at $-20°C$ in darkness resulted in an overall recovery of $> 80\%$ compared to the freshly measured samples for AHLs, except for C14 (68%) and OXO6 (53.5%) (Supporting Information Fig. S4). This result demonstrates the reliability of the analytical protocol and the stability of these compounds under the selected conditions.

The recoveries measured for the ISTDs after DCM extraction demonstrated that this extraction method is suitable for nonfunctionalized AHLs but less so for AHLs containing a hydroxyl- or a keto-group (Supporting Information Fig. S5). The recovery for C8D ranged from 6% to 41% and for C12D from 13% to 47% while very low recoveries were observed with OXO9 (3–6%) and no recovery was observed for OH13. While these values are low compared to liquid extraction performed with ethyl acetate on pure bacterial cultures (Ortori et al. 2011), they are comparable to values from field samples extracted with methanol (Sun et al. 2018) and only slightly lower compared to samples extracted with solid phase extraction techniques (Wang et al. 2017).

In our study, samples were evaporated using a RapidVap system which allowed evaporation of several samples simultaneously but has a lower evaporation rate compared to a rotary evaporator. Therefore, we chose DCM as volatile extraction solvent to decrease the evaporation time as much as possible to avoid AHL degradation, resulting in an acceptable compromise between extraction efficiency and evaporation time.

AHL content of intertidal sediments

Sediment samples were extracted with DCM and analyzed for their AHL content using UHPLC-HRMS to evaluate whether our sampling and extraction protocol was applicable. We focused on AHLs with even-numbered acyl-side chains in this study because the fatty acids utilized in AHL synthesis commonly have even-numbered carbon chains (Parsek et al. 1999). Out of the 15 AHL standards with even numbered acyl side chains (C6–C14, OH6–OH14, and OXO6–OXO14), eight could be identified in sediment samples in more than one replicate (C8, C10, C12, OH10, OH12, OH14, OXO10, and OXO12) and three AHLs could be quantified (C8, C10, and C12) (Table 3). More polar compounds like C6, OH6, OXO6, OH8, and OXO8 were not detected in the sediments. Among the identified AHLs, C12 and C8 were the most abundant ones and were found in $> 70\%$ of all samples. OXO12, OH12, and C10 were detected in 30–70% of the samples and OH14, OH10, and OXO10 in less than 30% (Table 3). Regarding their quantification, the AHLs C8 and C12 were present at the highest concentrations (average 181 and 76 ppb) followed by considerably lower concentrations of C10 (average 0.9 ppb). Among these three AHLs, we did not observe strong differences between sampling seasons regarding their concentration and frequency of occurrence (Fig. 6).

Discussion

Intertidal mudflats represent an environment where microorganisms such as diatoms and bacteria are densely packed within the photic zone of the sediment. Despite the increasing body of work indicating that AHLs play an underestimated role in algae-bacteria interactions, so far only very few studies have attempted to quantify in situ AHL concentrations in ecologically relevant systems. This is likely due to the technical difficulties associated with sampling, extraction, identification, and quantification of AHLs. To address these challenges, this study aimed to identify and quantify a set of target AHLs present in low concentrations in intertidal sediments and provides a new approach for sediment sampling and subsequent AHL quantification.

Intertidal mudflats are highly productive areas in terms of primary production and often covered by diatom-dominated biofilms (Underwood and Kromkamp 1999; Van Colen et al. 2014). As no described sampling method was suitable to collect the photic zone of the sediment for AHL extraction, we used a sampling method that was already successfully implemented to collect microphytobenthos for DNA and pigment extractions (Maris and Meire 2017). To our knowledge, this is the first demonstration of sampling with contact cores to analyze natural products from intertidal sediments besides pigments and nucleic acids. The method is robust and the amount of sediment allowed us to not only determine AHL concentrations but also to collect meta data such as TOM content and grain size in the same sample. Compared to a previously described method by Huang et al. (2007), sediment sampling with contact cores was less time-intensive and did not select for settlers on an artificial substrate. In addition, the bottom depth of the contact core ensured that only the euphotic zone (top 2 mm) of the sediment was sampled where the majority of the microalgal biomass is located (Forster and Kromkamp 2004).

Furthermore, we developed a fast and robust UHPLC-HRMS method, which achieved a baseline separation of a higher number of AHLs compared to other published methods (Ortori et al. 2011; Wang et al. 2017) and allowed to unambiguously identify most of the investigated AHLs in TIC mode. All AHLs were accessible in selected-ion monitoring mode and the high sensitivity of the Orbitrap analyzer made it possible to quantify compounds that were present at low abundances with an unprecedented accuracy. HRMS provided the accurate mass to reliably identify each AHL, even when AHLs were not perfectly baseline separated. Thanks to MS^2 experiments, the accurate mass of the characteristic lactone ring fragment ion

Table 3. *N*-acyl homoserine lactones detected in all sediment samples (*n* = 33). Concentrations were calculated based on the sum of both parent ions, [M + H] + and [M + Na] + with "n.q." = not quantified. Identifications describe the number of samples in which an AHL was identified and relative abundance the respective percentage (33 = 100%). Relative abundances are provided as *** = very common (70–100%), ** = common (30–70%), and * = less common (0–30%). Table was adapted according to Decho et al. (2009).

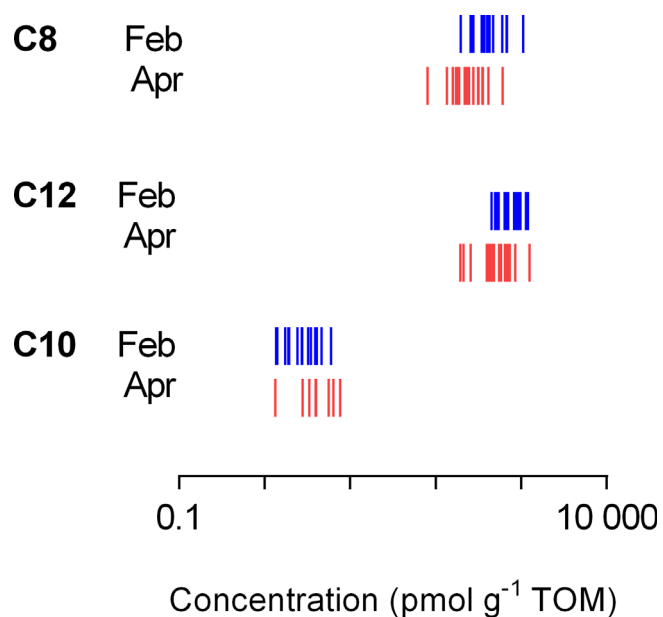| AHL	Parent ions		Concentration		Identifications	Rel. abundance
	$[M + H]^+$	$[M + Na]^+$	$[pmol\ g^{-1}\ TOM]$	[ppb]		
C12	284.2216	306.2034	640.4±258.4	181.4±73.2	33	***
C8	228.1592	250.1411	335.6±201.6	76.3±45.8	32	***
C10	256.1903	278.1722	3.5±1.7	0.9±0.4	22	**
OXO12	298.2007	320.1825	n.q.	n.q.	14	**
OH12	300.2165	322.1982	n.q.	n.q.	14	**
OH14	328.2476	350.2294	n.q.	n.q.	4	*
OH10	272.1853	294.1671	n.q.	n.q.	3	*
OXO10	270.1697	292.1514	n.q.	n.q.	3	*

Fig 6. AHL concentrations of C8, C12, and C10 (blue = February, red = April). Each replicate is plotted individually on a logarithmic scale.

(*m/z* = 102.0549) could be monitored providing additional proof for correct identification. Moreover, performing nontargeted MS[2] experiments, such as AIF over the entire chromatographic profile without preselecting a precursor mass, and searching for the accurate mass of the lactone ring fragment ion provides a tool to identify nonstandard AHLs with unknown retention times, for example, AHLs with odd numbered acyl chains like *N*-heptanoyl homoserine lactone (C7) which was previously identified in microbial mats (Decho et al. 2009). Looking at AIF chromatograms, we could find peaks corresponding to the lactone ring fragment ion that did not correspond to our standards (e.g., peaks at 5.72, 8.84, and 9.84 min, Supporting Information Fig. S6). However, due

to the low concentration of these compounds and the high matrix effect, a complete identification of these putative AHLs was not possible. Still, this technique, together with the use of different solvents and solvent mixtures for AHL extraction, an additional purification step and a higher amount of sample, would significantly extend the possibility of finding novel AHLs. Precise quantification will, however, only be possible with the use of authentic internal standards due to variable extraction success and ionization efficiency. The analytical method presented in this study is thus applicable to AHLs present at low concentrations in complex matrices and can be utilized as is for AHL detection in environmental samples.

For AHL quantification, TOM content of each sample was used as a parameter for normalization, whereas previous studies predominantly used air- or freeze-dried weight of biofilms or sediment. Even though this procedure adds one step to the AHL quantification, that is, ashing of sediment, it was useful to make AHL concentrations in different sediments comparable which naturally have a high variation in biomass (Herman et al. 2001). In previous studies samples often consisted almost entirely of biomass, for example, sludge or microbial mats, and most of the dry weight of these samples was composed of organic matter making ashing of the sample obsolete (Decho et al. 2009; Wang et al. 2017).

Regarding the AHL extraction from the sediment samples, we adapted a method with DCM which has been used in the past to quantify AHLs from microbial mats (Decho et al. 2009). However, recovery rates for pure standards were comparably low and showed that apolar AHLs (C8D and C12D) were extracted with higher efficiency compared to polar compounds (OXO9 and OH13). Despite this drawback, DCM extraction was considered as an acceptable trade-off between extraction efficiency and evaporation time, making processing faster than many other extraction methods described to date. Higher extraction efficiencies for apolar compounds indicated that DCM extraction was likely to

introduce a bias in the AHL identification which would explain why hydrophobic AHLs like C12 and C8 were identified with the highest signal intensities. However, normalization prevents a bias in concentration and the prevalence of apolar AHLs is in accordance with the literature (Decho et al. 2009; Wang et al. 2017). For example, Decho et al. (2009) identified highest concentrations for C8 and C10 in microbial mats and Wang et al. (2017) found highest concentrations for C10 and C12 in wastewater treatment biofilms using ethyl acetate for extraction.

Along with different extraction efficiencies, it should be noted that AHLs can be modified by environmental factors leading to hydrolysis or oxidation of the molecules (Decho et al. 2011). Due to their high photosynthetic rates, phototrophic biofilms often have alkaline pH conditions during daytime which favor hydrolysis, a reaction which leads to ring opening of the lactone moiety of the AHL (Decho et al. 2011). On the other hand, reactive oxygen species are often produced as byproducts of photosynthesis which could spontaneously oxidize AHLs giving rise to nonspecific oxidized AHL analogues (Decho et al. 2011). Thus, our study might underestimate the AHL concentration in phototrophic microbial communities due to hydrolysis while oxidized AHLs, that is, 3-oxo-AHLs and hydroxylated AHLs, might also be products of oxidation processes.

Nevertheless, this study presents an effective approach to sample, extract, and quantify AHLs from intertidal sediments. The sampling method is easy to carry out in the field and ensures that only the top 2 mm of the sediment are sampled. The described extraction method with DCM is a compromise between extraction efficiency and evaporation time. Compared to the extraction method by Decho et al. (2009), our extraction method is faster and the recovery rates for acyl AHLs are comparable to other studies which utilized different solvents. If polar AHLs are targeted, the extraction can be adapted by using more polar solvents or solvent mixtures. An additional solid phase extraction step can be easily introduced in the extraction workflow, especially when working with highly complex matrices. Compared to other analytical methods, our method presents a good compromise between short measurement time and peak separation, achieving baseline separation of a high number of AHL standards. In addition to the chromatographic performance, the use of HRMS allows to unambiguously identify known and potentially unknown AHLs even in complex matrices. All these characteristics make this methodology robust but also highly adaptable for AHL identification. Furthermore, the extraction solvents are easily exchanged to extract a broader range of compounds, thus expanding the potential of this sampling technique to other natural products.

References

Blott, S. J., and K. Pye. 2012. Particle size scales and classification of sediment types based on particle size distributions: Review and recommended procedures. Sedimentology **59**: 2071–2096.doi:10.1111/j.1365-3091.2012.01335.x

Bouma, T. J., and others. 2016. Short-term mudflat dynamics drive long-term cyclic salt marsh dynamics. Limnol. Oceanogr. **61**: 2261–2275.doi:10.1002/lno.10374

Brouwer, M. G. M., M. Wolthers, J. H. Hazeleger, F. Rossi, L. Lourens, J. Middelburg, and I. Duijnstee. 2015. Differential response of intertidal foraminifera to community recovery following experimentally induced hypoxia. J. Foraminifer. Res. **45**: 220–234.doi:10.2113/gsjfr.45.3.220

Cao, J. G., Z. Y. Wei, and E. A. Meighen. 1995. The lux autoinducer-receptor interaction in *Vibrio harveyi*: Binding parameters and structural requirements for the autoinducer. Biochem. J. **312**: 439–444.doi:10.1042/bj3120439

Churchill, M. E. A., and L. Chen. 2011. Structural basis of acyl-homoserine lactone-dependent signaling. Chem. Rev. **111**: 68–85.doi:10.1021/cr1000817

Decho, A. W., P. T. Visscher, J. Ferry, T. Kawaguchi, L. J. He, K. M. Przekop, R. S. Norman, and R. P. Reid. 2009. Autoinducers extracted from microbial mats reveal a surprising diversity of *N*-acylhomoserine lactones (AHLs) and abundance changes that may relate to diel pH. Environ. Microbiol. **11**: 409–420.doi:10.1111/j.1462-2920.2008.01780.x

Decho, A. W., R. L. Frey, and J. L. Ferry. 2011. Chemical challenges to bacterial AHL signaling in the environment. Chem. Rev. **111**: 88–99.doi:10.1021/cr100311q

Decleyre, H., K. Heylen, K. Sabbe, B. Tytgat, D. Deforce, F. Van Nieuwerburgh, C. Van Colen, and A. Willems. 2015. A doubling of microphytobenthos biomass coincides with a tenfold increase in denitrifier and total bacterial abundances in intertidal sediments of a temperate estuary. PLoS One **10**: e0126583. doi:10.1371/journal.pone.0126583

Doberva, M., S. Sanchez-Ferandin, E. Toulza, P. Lebaron, and R. Lami. 2015. Diversity of quorum sensing autoinducer synthases in the Global Ocean Sampling metagenomic database. Aquat. Microb. Ecol. **74**: 107–119.doi:10.3354/ame01734

Forster, R., and J. Kromkamp. 2004. Modelling the effects of chlorophyll fluorescence from subsurface layers on photosynthetic efficiency measurement in microphytobenthic algae. Mar. Ecol. Prog. Ser. **284**: 9–22.doi:10.3354/meps284009

Frederix, M., J. A. Downie, and R. K. Poole. 2011. Chapter 2 - quorum sensing: Regulating the regulators. Adv. Microb. Physiol. **58**: 23–80.doi:10.1016/B978-0-12-381043-4.00002-7

Herlory, O., J. M. Guarini, P. Richard, and G. F. Blanchard. 2004. Microstructure of microphytobenthic biofilm and its spatio-temporal dynamics in an intertidal mudflat (Aiguillon Bay, France). Mar. Ecol. Prog. Ser. **282**: 33–44. doi:10.3354/meps282033

Herman, P. M. J., J. J. Middelburg, and C. H. R. Heip. 2001. Benthic community structure and sediment processes on an intertidal flat: Results from the ECOFLAT project. Cont.

Shelf Res. **21**: 2055–2071.doi:10.1016/S0278-4343(01)00042-5

Hmelo, L. R. 2017. Quorum sensing in marine microbial environments. Ann. Rev. Mar. Sci. **9**: 257–281.doi:10.1146/annurev-marine-010816-060656

Hodgkinson, J. T., W. R. J. D. Galloway, M. Casoli, H. Keane, X. Su, G. P. C. Salmond, M. Welch, and D. R. Spring. 2011. Robust routes for the synthesis of *N*-acylated-L-homoserine lactone (AHL) quorum sensing molecules with high levels of enantiomeric purity. Tetrahedron Lett. **52**: 3291–3294. doi:10.1016/j.tetlet.2011.04.059

Huang, Y. L., S. Dobretsov, J. S. Ki, L. H. Yang, and P. Y. Qian. 2007. Presence of acyl-homoserine lactone in subtidal biofilm and the implication in larval behavioral response in the polychaete *Hydroides elegans*. Microb. Ecol. **54**: 384–392.doi:10.1007/s00248-007-9210-9

Joint, I., K. Tait, and G. Wheeler. 2007. Cross-kingdom signalling: Exploitation of bacterial quorum sensing molecules by the green seaweed *Ulva*. Philos. Trans. R. Soc. Lond. B Biol. Sci. **362**: 1223–1233.doi:10.1098/rstb.2007.2047

Li, Z., and S. K. Nair. 2012. Quorum sensing: How bacteria can coordinate activity and synchronize their response to external signals? Protein Sci. **21**: 1403–1417.doi:10.1002/pro.2132

Maris, T., and P. Meire. 2017. Onderzoek naar de gevolgen van het Sigmaplan, baggeractiviteiten en havenuitbreiding in de Zeeschelde op het milieu. Geïntegreerd eindverslag van het onderzoek verricht in 2016. Universiteit Antwerpen.

Miller, J. N., and J. C. Miller. 2005. Statistics and chemometrics for analytical chemistry. Pearson Education.

Natrah, F. M. I., M. M. Kenmegne, W. Wiyoto, P. Sorgeloos, P. Bossier, and T. Defoirdt. 2011. Effects of micro-algae commonly used in aquaculture on acyl-homoserine lactone quorum sensing. Aquaculture **317**: 53–57.doi:10.1016/j.aquaculture.2011.04.038

Ortori, C. A., J. -F. Dubern, S. R. Chhabra, M. Cámara, K. Hardie, P. Williams, and D. A. Barrett. 2011. Simultaneous quantitative profiling of N-acyl-l-homoserine lactone and 2-alkyl-4(1H)-quinolone families of quorum-sensing signaling molecules using LC-MS/MS. Anal. Bioanal. Chem. **399**(2): 839–850. doi:10.1007/s00216-010-4341-0.

Parsek, M. R., D. L. Val, B. L. Hanzelka, J. E. Cronan Jr., and E. P. Greenberg. 1999. Acyl homoserine-lactone quorum-sensing signal generation. Proc. Natl. Acad. Sci. USA **96**: 4360–4365.doi:10.1073/pnas.96.8.4360

Ruysbergh, E., C. V. Stevens, N. De Kimpe, and S. Mangelinckx. 2016. Synthesis and analysis of stable isotope-labelled *N*-acyl homoserine lactones. RSC Adv. **6**: 73717–73730.doi:10.1039/c6ra17797b

Sheng, H., Y. Song, Y. Bian, W. Wu, L. Xiang, G. Liu, X. Jiang, and F. Wang. 2017. Determination of *N*-acyl homoserine lactones in soil using accelerated solvent extraction combined with solid-phase extraction and gas chromatography-mass spectrometry. Anal. Methods **9**: 688–696.doi:10.1039/C6AY02652D

Steindler, L., and V. Venturi. 2007. Detection of quorum-sensing *N*-acyl homoserine lactone signal molecules by bacterial biosensors. FEMS Microbiol. Lett. **266**: 1–9.doi:10.1111/j.1574-6968.2006.00501.x

Stock, F., and others. 2019. *N*-acyl homoserine lactone derived tetramic acids impair photosynthesis in *Phaeodactylum tricornutum*. ACS Chem. Biol. **14**: 198–203.doi:10.1021/acschembio.8b01101

Sun, Y., K. He, Q. Yin, S. Echigo, G. Wu, and Y. Guan. 2018. Determination of quorum-sensing signal substances in water and solid phases of activated sludge systems using liquid chromatography–mass spectrometry. J. Environ. Sci. **69**: 85–94.doi:10.1016/j.jes.2017.04.017

Syrpas, M., E. Ruysbergh, L. Blommaert, B. Vanelslander, K. Sabbe, W. Vyverman, N. De Kimpe, and S. Mangelinckx. 2014. Haloperoxidase mediated quorum quenching by *Nitzschia cf pellucida*: Study of the metabolization of *N*-acyl homoserine lactones by a benthic diatom. Mar. Drugs **12**: 352–367.doi:10.3390/md12010352

Teplitski, M., and others. 2004. *Chlamydomonas reinhardtii* secretes compounds that mimic bacterial signals and interfere with quorum sensing regulation in bacteria. Plant Physiol. **134**: 137–146.doi:10.1104/pp.103.029918

Underwood, G. J. C., and J. Kromkamp. 1999. Primary production by phytoplankton and microphytobenthos in estuaries. Adv. Ecol. Res. **29**: 93–153.doi:10.1016/S0065-2504(08)60192-0

Van Colen, C., G. J. C. Underwood, J. Serodio, and D. M. Paterson. 2014. Ecology of intertidal microbial biofilms: Mechanisms, patterns and future research needs. J. Sea Res. **92**: 2–5.doi:10.1016/j.seares.2014.07.003

Van Heukelem, L., and C. S. Thomas. 2001. Computer-assisted high-performance liquid chromatography method development with applications to the isolation and analysis of phytoplankton pigments. J. Chromatogr. A **910**: 31–49.doi:10.1016/S0378-4347(00)00603-4

Wagner-Döbler, I., and others. 2005. Discovery of complex mixtures of novel long-chain quorum sensing signals in free-living and host-associated marine alphaproteobacteria. ChemBioChem **6**: 2195–2206.doi:10.1002/cbic.200500189

Wang, J., L. Ding, K. Li, W. Schmieder, J. Geng, K. Xu, Y. Zhang, and H. Ren. 2017. Development of an extraction method and LC–MS analysis for N-acylated-l-homoserine lactones (AHLs) in wastewater treatment biofilms. J. Chromatogr. B **1041-1042**: 37–44. doi:10.1016/j.jchromb.2016.11.029.

Waters, C. M., and B. L. Bassler. 2005. Quorum sensing: Cell-to-cell communication in bacteria. Annu. Rev. Cell Dev. Biol. **21**: 319–346.doi:10.1146/annurev.cellbio.21.012704.131001

Winson, M. K., and others. 1998. Construction and analysis of luxCDABE-based plasmid sensors for investigating *N*-acyl homoserine lactone-mediated quorum sensing. FEMS Microbiol. Lett. **163**: 185–192.doi:10.1111/j.1574-6968.1998.tb13044.x

Yang, C., S. Fang, D. Chen, J. Wang, F. Liu, and C. Xia. 2016. The possible role of bacterial signal molecules *N*-acyl homoserine lactones in the formation of diatom-biofilm (*Cylindrotheca* sp.). Mar. Pollut. Bull. **107**: 118–124.doi:10.1016/j.marpolbul.2016.04.010

Zhou, J., Y. Lyu, M. L. Richlen, D. M. Anderson, and Z. Cai. 2016. Quorum sensing is a language of chemical signals and plays an ecological role in algal-bacterial interactions. Crit. Rev. Plant Sci. **35**: 81–105.doi:10.1080/07352689.2016.1172461

Zhu, J., Y. R. Chai, Z. T. Zhong, S. P. Li, and S. C. Winans. 2003. *Agrobacterium* bioassay strain for ultrasensitive detection of *N*-acylhomoserine lactone-type quorum-sensing molecules: Detection of autoinducers in *Mesorhizobium huakuii*. Appl. Environ. Microbiol. **69**: 6949–6953.doi:10.1128/aem.69.11.6949-6953.2003

Conflict of Interest

None declared.